

# Deep Learning in Simulation of Nickel-based Superalloys Ultimate Tensile Strength: Accounting the Role of Alloying Elements

ANDREY TYAGUNOV, OLEG MILDER, DMITRY TARASOV

Department of IT and Automation

Ural Federal University

Mira 32 – R041, Ekaterinburg 620002

RUSSIA

datarasov@yandex.ru <http://www.urfu.ru>

*Abstract:* - Nickel-based superalloys are unique high temperature materials with complex doping used for the gas turbine engines parts and other heat-resistant devices manufacturing, which makes them extremely important for the industry. The alloys exhibit excellent resistance to mechanical and chemical degradation under high loads and long-term isothermal exposures. One of the main service property of the superalloys is the ultimate tensile strength (UTS) or creep to rupture that is measured after the alloy sample is heated to a certain temperature and is held for a certain (prolonged) time. The common design of new alloys is time and money consuming. In particular, given the circumstances of the lack of information on the complete set of studied times and temperatures. Computational modeling would significantly simplify this process. In our work, we have applied a method of deep learning for modeling the superalloys UTS based on preliminary knowledge of their compositions, information on the role of alloying elements, solidification type, crystallographic direction of crystallization, test temperatures and exposure times, and the known UTS values. The simulation shows good agreement with the experimental data.

*Key-Words:* - nickel-based superalloys, artificial neural network, ultimate tensile strength, heat resistance, deep learning

## 1 Introduction

Nickel-based superalloys is a family of special heat resistant materials designed for the manufacture of critical parts of turbine engines. The matrix of the alloys is formed by nickel as an isomorphic material. The doping engages dozen other elements including Cr, Co, Mo, W, Al, Ti, *etc.* and even exotic Re, Ru, Hf. The time-dependent mechanical properties of the alloys are represented by a number of parameters determined as a result of various tests, however, among them, one can be highlighted, which determines the ultimate capabilities of a particular alloy before its failure at a given temperature, exposure time and working conditions. It is the ultimate tensile strength (UTS, MPa), that values are denoted as  $\sigma_t^\tau$ , where  $\tau$  is the exposure time (in hours), and  $t$  is the temperature (in °C) [1–5].

The issues of alloy and components design, process development, life expectancy, and material behavior are closely interrelated. In order to increase their mechanical properties, doping of the alloys is carried out. Some of the alloying elements are used to strengthen the nickel matrix by creating a solid solution. The other part forms excess phases:

intermetallides, carbides and borides. The roles of alloying elements in superalloys are shown in Table 1[1, p29].

In the alloys, under operating conditions at elevated temperatures, the hardening phases dissolve and embrittlement is released. The later this occurs, the more heat-stable the alloy is. Frequently, new alloy compositions with sufficiently high initial heat resistance are not stable and lose their properties. The first generations of alloys were created by equiaxial polycrystalline casting. Modern alloys use directional solidification and even high-tech single-crystal casting.

Synthesis of new superalloys has always been based on knowledge of the behavior of alloying elements, their participation in the formation of structural components, and their contribution to the complex of product properties.

Often, the role of alloying elements is considered individually, which generates a lot of conflicting information. The analysis of the effect of the chemical composition on the product properties is an entangled and multidimensional task.

It can be argued that there are a lot of factors affecting the properties of alloys. Thus, the issues of

new alloys modeling are complex tasks that are usually associated with a large number of expensive experiments, which, moreover, take a fair amount of time.

TABLE 1. Role of alloying elements in superalloys

Effect	Alloying elements
Solid-solution strengtheners	Co, Cr, Fe, Mo, W, Ta, Re
Carbide form MC	W, Ta, Ti, Mo, Nb, Hf
Carbide form M <sub>7</sub> C <sub>3</sub>	Cr
Carbide form M <sub>23</sub> C <sub>6</sub>	Cr, Mo, W
Carbide form M <sub>6</sub> C	Mo, W, Nb
Carbonitrides: M(CN)	C, N
Forms $\gamma'$ Ni <sub>3</sub> (Al, Ti)	Al, Ti
Raises solvus temperature of $\gamma'$	Co
Hardening precipitates and/or intermetallics	Al, Ti, Nb
Oxidation resistance	Al, Cr, Y, La, Ce
Improve hot corrosion resistance	La, Th
Sulfidation resistance	Cr, Co, Si
Improves creep properties	B, Ta
Increases rupture strength	B*
Grain-boundary refiners	B, C, Zr, Hf
Retard coarsening	Re

\* if present in large amounts, borides are formed

Today, more and more often, instead of natural modeling of the alloys properties, various mathematical models are applied. However, up to date, there is no unified model that describes the behavior of the alloys with a specific composition under various test conditions. The most frequently used models are various statistical ones. Moreover, since the behavior of the alloys properties often non-linear, the statistical approach based on utilization of artificial neural networks (ANN) is considered the most promising since the neural networks models have proven to be a great tool that are able to

simulate significant non-linearity [6]. Such attempts have shown promising results [7].

In this work, we extend the ANN approach to predict UTS of superalloys based on the knowledge of their compositions, the role of alloying elements (see Table 1), and the known UTS values. For modeling, we apply the deep learning artificial neural network (DLANN), which is built in Matlab. Such, we predict the unknown UTS values and form the general picture of alloying elements contribution into the alloys properties. In addition, we compare the obtained results with the preliminary ANN models and with known experimental data. For the model results assessment, as the independent alloys group, we use a set of common superalloys with at least five known UTS values. For the verification by calculating the errors between the real and predicted values, we extracted six common superalloys from the database that form such a group (see Table 2).

## 2 Approach and Experimental

To build the model, we first had to collect a database on the nickel-based superalloys. This database has been collecting for three years and is still being replenished. For the modeling, we use a sample of 300 superalloys (Russian and Western made) with known chemical composition. Data on alloys were collected from open sources (articles, catalogues, patents, theses). Some alloys from the sample have information on at least 5 results of testing (time  $\tau$ , temperature  $t$ , and UTS) for each alloy, and some not.

The conditions and results of the tests formed 2,200 individual samples in the database, which later served as input data for neural networks training. Each known result of the UTS tests under certain conditions of the isothermal exposure forms one sample.

For the visualization of results, we combine the test time and temperature conditions in one complex Larson-Miller parameter ( $P_{LM}$ ) (1) in the assumption that the absolute temperature  $T=t+273$ . In order to improve the information content of the database and to facilitate comparison of the test results for the

TABLE 2. Chemical compositions of some common cast superalloys, wt% (Ni is balanced)

Alloy	Cr	Co	Mo	W	Al	Ti	Nb	Ta	Re	Ru	Hf	C	B	Zr
CMSX-4	6.5	9.0	0.6	6.0	5.6	1.0	-	6.5	3.0	-	0.1	-	-	-
PWA1480	10.0	5.0	-	4.0	5.0	1.5	-	12.0	-	-	-	-	-	-
RENE N5	7.0	8.0	2.0	5.0	6.2	-	-	7.0	3.0	-	0.2	-	-	-
IN100	10.0	15.0	3.0	-	5.5	4.7	-	-	-	-	-	0.18	0.004	0.06
MAR-M247	8.0	10.0	0.6	10.0	5.5	1.0	-	3.0	-	-	1.5	0.15	0.015	0.03
MC-NG	4.0	-	1.0	5.0	6.0	0.5	-	5.0	4.0	4.0	0.1	-	-	-

heat resistance, we have modified  $P_{LM}$  by division by  $10^5$  in order to obtain values of the same dimension as the alloying elements concentrations do (decimal format with values between 0 and 1). Moreover, the alloying elements concentrations in the database have been normalized to the nickel concentration.

$$P_{LM} = T \times (20 + \lg \tau) \times 10^{-5} . \quad (1)$$

Since the UTS range in experiments covers a band of several orders of magnitude, we use its logarithmic transformation (2) that, also, makes prediction errors relative. Moreover, the model target values ( $y$ ) for the inverse transformation (3) exclude the possibility of negative  $\sigma$  values, which are physically impossible. All this improves the performance of the model.

$$y = \lg \sigma \quad (2)$$

$$\sigma = 10^y \quad (3)$$

The previous works [8–15] related to the modelling of superalloys features and behaviour used different types of feed-forward artificial neural networks. Previously, we have shown that the Bayesian regularized artificial neural network (BRANN) not only more robust than standard back-propagation ones and is able to reduce or even eliminate the need of cross-validation, but it has shown satisfactory predictive ability along with resistance to overtraining in the superalloys UTS modelling [7].

However, the need to take into account a large number of unequal alloying elements requires a more complex model organization. In order to improve accuracy of the model, we also engaged the information on the solidification type of each alloy (equiaxed casting, direct solidification, single-crystal casting). These data are implicitly related to the composition of the alloys, but directly form their mechanical properties.

The deep learning approach, where each layer of the neural network is responsible for its own set of properties, makes it possible to account a large number of diverse input parameters forming a non-linear statistical model.

The deep learning framework is based on the interconnection matrix (Table 3) that define the linkages between the input layer and the first layer of hidden neurons. The matrix reflects the major metallurgical phase components, as well as, the solidification type forming a particular hidden layer.

To create and train the DLANN, the MATLAB 2014a software package with the built-in MATLAB *nntools* was used. To improve the accuracy of simulations, a specially developed bootstrap algorithm. The configuration of the network is shown in Fig.1.

The network is a non-fully connected perceptron, in which separate groups of neurons of the first hidden layer are responsible for the specific role of the alloying elements in accordance with Tables 1 and 3. Such, for example, C and Cr participate in the formation of  $M_7C_3$  carbides and are inputs of the corresponding group of neurons. On the other hand, each of the groups named in Table 3 is internally

TABLE 3. Interconnection matrix for DLANN, “1” means the presence of a linkage

Roles of alloying elements	C	Cr	Co	Mo	W	Al	Ti	Nb	B	Fe	Zr	Ta	Re	Ru	V	Ce	La	S	Si	Mn	P	Hf	CV <sup>1</sup>	
SSH <sup>2</sup>		1	1	1	1					1		1	1	1									1	
MC <sup>3</sup>	1			1	1	1	1					1			1								1	1
M <sub>7</sub> C <sub>3</sub>	1	1																					1	
M <sub>23</sub> C <sub>6</sub>	1	1		1	1																		1	
M <sub>6</sub> C	1			1	1			1															1	
$\gamma'$						1	1	1				1										1	1	
OxRes <sup>4</sup>		1				1										1	1						1	
S_Res <sup>5</sup>		1	1				1												1				1	
Im_Crp <sup>6</sup>									1			1											1	
Gr_Bnd <sup>7</sup>	1								1		1											1	1	
GPR <sup>8</sup>													1	1									1	
Tsld_Up <sup>9</sup>					1								1										1	
Rest <sup>10</sup>																		1		1	1		1	
Out <sup>11</sup>	1		1						1														1	

<sup>1</sup> CV is the 6D Casting Vector combining the solidification type, crystallographic direction of crystallization (3 components), test time ( $\tau$ ), and test temperature ( $T$ ); <sup>2</sup> SSH is the solid solution hardening; <sup>3</sup> M<sub>x</sub>C<sub>y</sub> are carbides; <sup>4</sup> is the oxidation resistance; <sup>5</sup> is the sulfidation resistance; <sup>6</sup> improves creep properties; <sup>7</sup> are grain-boundary refiners; <sup>8</sup> retard  $\gamma'$  coarsening; <sup>9</sup> increases solidus temperature; <sup>10</sup> rest impurities; <sup>11</sup> connections to the output

fully connected. The transfer function in use is than-sigmoid. Then, the 6-dimensional Casting Vector (CV) combining the solidification type, crystallographic direction of crystallization (3 components), test time ( $\tau$ ), and test temperature ( $T$ ) is fed to the input of each of the groups.

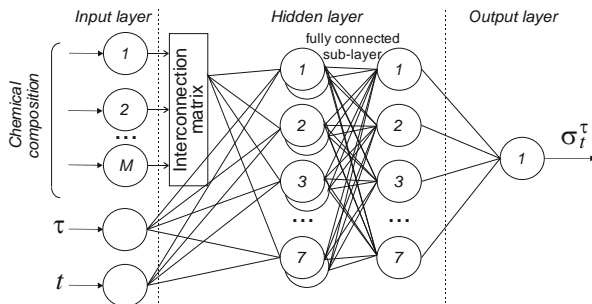


Fig. 1. DLANN configuration

The network training procedure is the error back propagation with Bayesian regularization. In order to avoid overtraining, not very strict training parameters (the target minimum error (MSE) (5) and the gradient) were empirically selected.

$$MSE = \frac{\sum_{i=1}^n (y_{predicted,i} - y_{fact,i})^2}{n} \quad (5)$$

The bootstrap is described as follows. In each training iteration, the input data vary based on a quintile decomposition of the input database. For the training cycle, only randomly selected 90% of initial data are applied. The rest 10% are applied for the model validation at the final stage. At each iteration, the formed dataset (90%) is randomly divided into the training (75%) and the test (25%) sub-samples that are involved in training.

The stop criterion for the iteration is the desired level of mean squared error (MSE) (5) achieved during the training. The target MSE value is chosen empirically and is set slightly below the level at which the MSE of training and test samples obtained after the next training epoch begin to diverge. In our case, based on preliminary study, we selected the following criterion:  $MSE.test \geq 1.2 \times MSE.training$ .

Thus, after numerous experiments, an artificial neural networks set with the highest accuracy of prediction ( $MSE = 3 \times 10^{-4}$ ) has been achieved.

The framework's prediction ability is evaluated by the related root mean squared error (RRMSE) between the DLANN predictions and the real data from the validation sub-sample (10%).

As the model independent assessment, we engage the verification group (Table 2). Using the experimental and reconstructed values of the UTS for the alloys from the group, we plotted the

dependences of the UTS vs the Larson-Miller parameter.

$$RRMSE = \sqrt{\frac{\sum_{j=1}^k \left( \frac{\sigma_{predicted,j} - \sigma_{real,j}}{\sigma_{real,j}} \right)^2}{k}} \quad (6)$$

The heterophasic structure of the alloys manifests itself in multistage degradation under the influence of temperature and pressure due to the different thermal stability of the structural components. This is also reflected in the significant nonlinearity of the dependence of the UTS on the parameter. The observed asymptotic tendencies toward stabilization of the UTS at values of the Larson-Miller parameter approximately below 20 and above 30, as well as, an almost linear decrease in the UTS within the indicated range, suggest that such a dependence can be described by a sigmoid function of the form (7).

$$\sigma(x) = \sigma_2 + \frac{\sigma_1 - \sigma_2}{1 + \exp\left(\frac{x - x_0}{p}\right)} \quad (7)$$

were  $\sigma_1, \sigma_2, x_0, p$  are the parameters that are established during the approximation:  $\sigma_1, \sigma_2$  are the asymptotes of almost constant  $\sigma$ ,  $x_0$  is a center (inflection point) of the sigmoid, and  $p$  is a slope factor that is numerically indicates the range of  $P_{LM}$  where the function (7) decreases between  $\sigma_1$  and  $\sigma_2$  levels and, thus, reflects the thermo-temporal dynamics of the alloys phase stability. Such an approximation of the observed dependences is much more physical than the usually used linear one.

### 3 Results and Discussion

On the basis of the Deep Learning Artificial Neural Network, a model for simulation UTS of nickel-based superalloys has been created and tested.

The model UTS (calculated at the validation 10% sub-sample) prediction errors (RRMSE) distribution is shown in Fig.2. As it can be seen, the error do not exceed 0.40 for most observations, moreover, the median value is 0.09 and 75% percentile is 0.17. Thus, we can assume that the model performance is satisfactory.

The model UTS predictions together with the real experimental data and with approximations by (7) for six common superalloys from the verification group (see Table 1) are shown in Fig.3. In the final fully filled database, the modelled results have not been combined with the real test data. They were placed separately in order to improve the overall model accuracy. Thus, it is impossible to compare real and predicted data directly. Despite the absence

of numerical evaluation of the errors, Figure 3 shows the satisfactory accuracy of the both, the DLANN predictions and the sigmoidal approximation.

The model gives less accuracy in the area of low  $P_{LM}$  since they are related to either short test exposures or low test temperatures. These data usually is not presented in the literature sources forming the initial database. This, also, lead to a scatter on the graphs of predictions (Fig.3) at the area of  $P_{LM}$  less than 24.

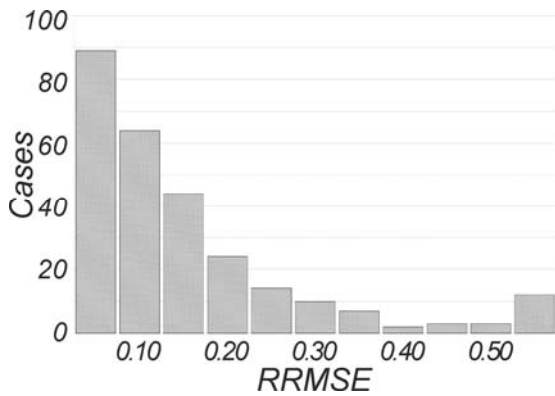


Fig. 2. The model predictions errors distribution

The simulated UTS values in the low  $P_{LM}$  region, in addition, are underestimated by about 7–10%. It is known that, for example, for the CMSX-4 superalloy, the short-time UTS is about 1100 MPa.

discrepancy insignificant, and the model will be further improved to refine forecasting by adding short-term UTS values to the initial database.

Analysing the sigmoidal approximations (Fig.3), we may deduce that the slope factor  $p$  not only characterizes how close the curves lay to the abscissa axis, moreover,  $p$  may act as an indirect indicator of the alloy thermal stability. The larger the  $p$ , the longer the structure resists degradation.

### 4 Conclusion

This paper has addressed the superalloys Ultimate Tensile Stress variation modelling by the Deep Learning Artificial Neural Network accounting different values of test temperature and exposure time combined in the Larson-Miller parameter.

The initial database for modelling has been formed by 300 superalloys with data on their known UTS values, chemical compositions, information on the role of alloying elements, as well as, the solidification type, crystallographic direction of crystallization, test temperatures and exposure times. It was such complexity that required the involvement of a sophisticated model of an artificial neural network.

The model has been built and trained in Matlab. The trained model exhibit the median value of RRMSE about 0.09, which is comparable with the magnitude of the error that is conventionally given

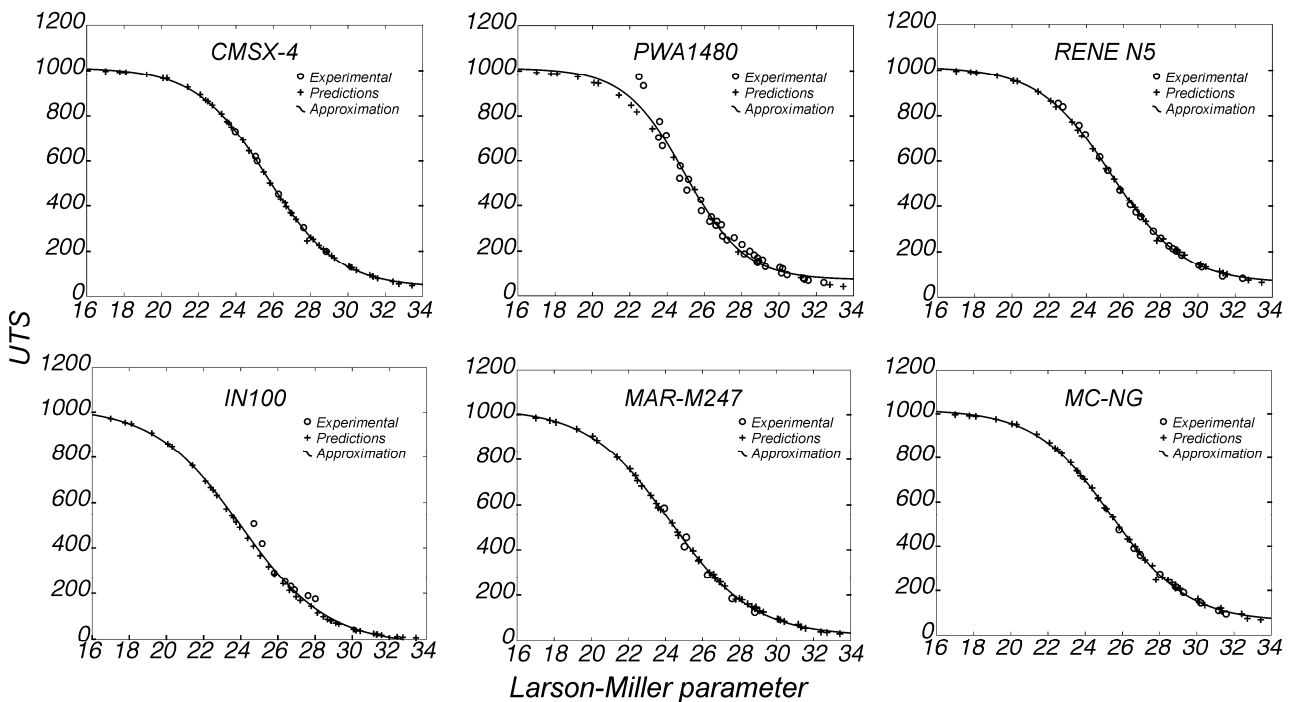


Fig.3. Calculated data on the effect of certain alloying elements on UTS of nickel superalloys

However, this area is usually not the subject of interest for researchers. Therefore, we consider this

in the reference literature on superalloys. The model verification has been carried out by predicting the

unknown UTS values for six common superalloys (Table 2) that did not take part in the model training.

Approximation of the  $\sigma(P_{LM})$  dependence by the sigmoid (eq. 7) has been done based on the supplemented data on UTS, and also taking into account the characteristic form of such a dependence with the asymptotes of constant  $\sigma$  values and the conditionally linear region of its variation in between.

The model verification and approximation have shown good predictive accuracy of the DLANN. Thus, these calculations have helped to obtain the dependences of the UTS on the Larson-Miller parameter. The results of the calculations coincide with the experimentally obtained data, which confirms the model adequacy. The approximation slope factor  $p$  characterises the thermal stability of the alloys.

#### References:

- [1] Donachie M. J., Donachie S. J. (2002) Super alloys: A Technical Guide, 2nd Edition. ASM International, 439p.
- [2] Kuznetsov V.P., Lesnikov V.P., Popov N.A. (2004) Structure and properties of the single-crystal high-temperature nickel alloy. UrFU. 160p. (In Russian).
- [3] Reed R.C. (2006) The super alloys. Fundamentals and applications, Cambridge, 388p.
- [4] Super alloys 2008 (2008) ed.by K.A.Green at al., TMS, Wiley, 1000p
- [5] Tyagunov A.G., Baryshev E.E., Stepanova N.N (2010) Influence of melt structure on the properties of Nickel based super alloys in the solid state. UrO RAN. 198p. (in Russian).
- [6] Haykin S.O. Neural Networks and Learning Machines, 3rd Ed. (2009) McMaster University, Ontario Canada. 906p.
- [7] Tyagunov A., Milder O., Tarasov D. (2019) Application of Artificial Neural Networks for Prediction of Nickel-based Super alloys Service Properties Based on the Chemical Composition. WSEAS Transactions on Environment and Development, Vol.15, 113–119.
- [8] Yoo Y.S., Kim I.S., Kim D.H., Jo C.Y., Kim H.M., Jone C.N. (2004) The application of neural network to the development of single crystal super alloys. Super alloys 2004. Edited by K.A. Green, T.M. Pollock, H. Harada, T.E. Howson, R.C. Reed, J.J. Schirra, and S. Walston TMS (The Minerals, Metals & Materials Society).
- [9] Muhammad H Hasan, Muataz Al Hazza, Mubarak W. ALGرافي, Zubair Imam Syed. (2014) ANN Modeling of Nickel Base Super Alloys for Time Dependent Deformation. Journal of Automation and Control Engineering Vol. 2, No.4. 353–356.
- [10] Nurgayanova O.S., Ganeev A.A. (2006) Mathematical modeling of the effect of alloying elements on the heat resistance of nickel alloys with a single crystal structure. Bulletin of Ufa State Aviation Technical University Vol. 8. № 4. 91–95. (In Russian)
- [11] Nurgayanova O.S., Ganeev A.A. (2006) Computer-aided design of cast nickel super alloys with a single-crystal structure. Polzunovskiy almanac. № 3. 22–26. (In Russian)
- [12] Nurgayanova O.S., Ganeev A.A. (2007) Neural network approaches to the design of new heat-resistant nickel casting alloys. Neurocomputers: development, application. № 10. 70–74. (In Russian)
- [13] Nurgayanova O.S., Ganeev A.A. (2007) Synthesis of cast nickel super alloys for castings with directional and single-crystal structure. Bulletin of Ufa State Aviation Technical University. Vol. 9. № 1. 160–169. (In Russian)
- [14] Burden F., Winkler D. (2008) Bayesian Regularization of Neural Networks. In: Livingstone D.J. (eds) Artificial Neural Networks. Methods in Molecular Biology, vol 458. Humana Press
- [15] Sydikhov A.S., Tyagunov A.G., Milder O.B., Ganeev A.A. (2019) ANN approach for Larson-Miller factor approximation in the space of alloy features. AIP Conference Proceedings 2116, 200015